Tracking and Analysis of FUCCI-Labeled Cells Based on Particle Filters and Time-to-Event Analysis

Kenji Fujimoto[1], Shigeto Seno[1*], Hironori Shigeta[1], Tomohiro Mashita[1, 2], Masaru Ishii[3, 4], Hideo Matsuda[1]

[1] Graduate School of Information Science and Technology, Osaka University, Suita, Osaka, Japan.
[2] Cybermedia Center, Osaka University, Toyonaka, Osaka, Japan.
[3] Graduate School of Medicine, Osaka University, Suita, Osaka, Japan.
[4] Graduate School of Frontier Bioscience, Osaka University, Suita, Osaka, Japan.

* Corresponding author. Tel.: +81-6-6879-4391; email: senoo@ist.osaka-u.ac.jp
Manuscript submitted November 30, 2019; accepted March 4, 2020.
doi: 10.17706/ijbbb.2020.10.2.94-109

Abstract: FUCCI (fluorescent ubiquitination-based cell cycle indicator) is a fluorescent probe used to visualize the cell cycle progression of individual cells using fluorescent proteins of different colors. Because the cell cycle is related to biological processes such as proliferation of cancer cells, analysis of imaging data visualized using FUCCI is extremely important. This paper proposes a method for spatiotemporal tracking and analysis of FUCCI-labeled cells from time-lapse videos. To address the color transition of the FUCCI-labeled cell with the cell cycle progression, the proposed method simultaneously estimates the location and the cell cycle phase of the target cell. Furthermore, to analyze the cell phase transition, this paper proposes to apply multistate time-to-event analysis to the information obtained through our tracking method. This paper demonstrates the usefulness of our method with application to FUCCI-labeled HuH7 cells (human hepatocellular carcinoma cell line).

Key words: Cell cycle, cell tracking, FUCCI, time-to-event analysis, particle filter.

1. Introduction

Recent advances in bioimaging technology have enabled the visualization of various biological processes, and automated systems for data acquisition have enabled high-throughput imaging. High-content screening (HCS), an imaging-based multi-parametric analysis method, is used in biological research and drug discoveries [1]. Such advances have been producing enormous amounts of data. Therefore, the development of algorithms for image quantification and analysis is an urgent issue.

We focus on cell cycle analysis of cells visualized using fluorescent ubiquitination-based cell cycle indicator (FUCCI) [2]. The cell cycle is a sequence of events in a cell, which starts when a cell is produced from its parent cell's division and finishes when the cell divides. The cell cycle is composed of four phases, i.e., gap 1 (G1), synthesis (S), gap 2 (G2), and mitosis (M). In the S phase, cells replicate their DNA to prepare for cell division in the M phase. The G1 and G2 phases are devoted to cell growth. FUCCI is a kind of fluorescent probe used to visualize phases in the cell cycle by staining cell nuclei with different fluorescence proteins according to the phase. Fig. 1 (a) shows FUCCI-labeled HuH7 cells (human hepatocellular carcinoma cell line) superimposed with red and green fluorescence on a corresponding differential interference contrast (DIC) microscopy image (gray). FUCCI cells emit red fluorescence in the G1 phase,

green fluorescence in the S and G2 phases, and no fluorescence in the M phase, as shown in Fig. 1 (b).

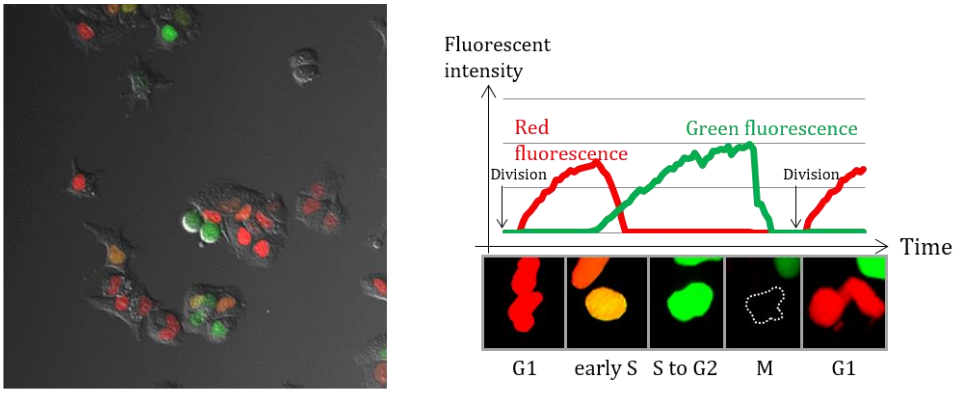

(a) FUCCI-labeled HuH7 cells (b) Fluorescence emission of FUCCI cells

Fig. 1. FUCCI and the cell cycle.

The cell cycle is known to be closely related to the proliferation of cancer cells, and some anti-cancer agents work specifically in the cell cycle. For example, topoisomerase inhibitors and antimetabolites are known to inhibit cancer cells from DNA replication in the S phase. Therefore, temporal observation of FUCCI-labeled cells (hereinafter referred to as FUCCI cells) in various conditions through time-lapse videos is important for evaluating medical efficacy and clarifying the response mechanism of anti-cancer agents. To extract information about cell cycle progression from such time-lapse videos, spatiotemporal tracking and phase estimation for each cell are required. FUCCI cell tracking can be a challenging task because the colors of the targets change according to the progress of the cell cycle, and the fluorescence signal of the targets disappears when cell division or cell death occurs. In FUCCI cell tracking, continuously tracking targets across different frames is more important than tracking many cells because the final goal is to analyze the relationship between time and cell cycle progression.

We propose a tracking method for FUCCI cells based on particle filters. A particle filter is a kind of time series filters and has been widely applied for target tracking problems because of its flexibility in describing the target's feature. To address the color transition of FUCCI cells according to the cell cycle progression, our method estimates the target's phase and utilizes it to localize the target in the next frame. In other words, for accurate tracking, our method simultaneously estimates the location and the cell cycle phase of the target cell interdependently. With the experimental result, we show that our method is suitable for FUCCI cell tracking compared to existing detection-based cell tracking methods. Furthermore, to show the usefulness of the information obtained through our method, we demonstrate the results of time-to-event (TTE) analysis to evaluate the effects of medicines on the cell cycle.

The rest of this paper is organized as follows. Section 2 introduces existing cell tracking methods. Section 3 proposes a method for tracking and extracting the phase of FUCCI cells and introduces TTE analysis for FUCCI cell data. Section 4 shows and discusses the results of experiments to evaluate our tracking methods and to verify the usefulness of data obtained through our method. Section 5 discusses our results and future work. Section 6 concludes this paper.

2. Cell Tracking

Cell tracking is a fundamental task for extracting dynamics from microscopy videos, and various methods have been proposed up to the present. Recently, deep learning-based tracking methods [3], [4] have achieved state-of-the-art performance. However, such methods require a sufficient number of training data,

which means pairs of video and target locations for each frame. Training data are created through manual annotation; thus, enough training data for experimental environments with a variety of targets, stains, and microscopes are usually not available. Therefore, we focus on tracking methods based on classical image processing.

Most existing cell tracking methods are detection-based methods. Detection-based methods perform segmentation (i.e., recognizing target regions and backgrounds in an image) to detect cells in each frame and associate the detected cells over frames. Some detection-based tracking methods, such as LineageTracker [5] and LAP (linear assignment problems) tracker [6], are capable of handling cell division, which frequently happens in FUCCI cell tracking. LineageTracker associates segmented regions based on the similarity of statistical features. This method detects cell division based on the fluorescence intensity and associates daughter cells with a parent cell that has the most similar statistical features. LAP tracker first performs frame-to-frame association of segmented regions. Then, this method links multiple trajectories obtained in the previous steps to close the gaps and capture division/fusion events. These steps are conducted via optimization of the cost functions (i.e., the dissimilarity between segmented regions or trajectories). These detection-based tracking methods heavily rely on the accurate segmentation. However, accurate segmentation for microscopic images can be a challenging task due to the low contrast, low S/N rate, and/or temporally weak fluorescence intensity. Therefore, detection-based tracking might produce multiple fragments of trajectories for each single cell. Because the purpose of FUCCI cell tracking is to analyze the cell cycle progression, continuously tracking the same cells for long time steps is extremely important, and fragmentation of trajectories might lead to wrong results of the following analyses.. As described above, LAP tracker has a gap-closing function to link fragments of trajectories and make the trajectories longer. Although, because LAP tracker's gap-closing function is based on the dissimilarity minimization, it is not suitable for cells with dynamic appearance changes such as FUCCI cells.

Other than detection-based cell tracking methods, various methods, such as particle filters [7], [8], image matching [9], and graph-based methods [10], have been proposed. Among these methods, particle filter-based methods are flexible for describing the features of the target. A particle filter [11] is a kind of time series filter based on sequential Bayesian estimation to predict the internal states of a system from the past observations. In particle filter-based target tracking, the internal state corresponds to the target location, and the observation corresponds to the sequence of frames. Each tracker represents the target location as a set of "particles" that are specific pixels around the target. In the first frame, each target is detected by some method, such as segmentation, and all particles belonging to each tracker are set at the center of the target. Then, each tracker iterates the procedures shown in Fig. 2 for each subsequent frame. To find the target in a frame, the tracker relocates particles from their locations in the previous frame by adding small displacements. Then, the tracker calculates the "likelihood" of each particle, which represents the possibility that the particle is in the target region and is based on the particle's local information, such as color. Particles with low likelihood (a certain percentage of them) are excluded, and the tracker samples new particles from the remaining particles with weights proportional to the likelihood to restore the number of particles. This procedure is called resampling. Then, the tracker relocates the particles in the next frame. The target location in each frame is calculated as the average location of particles weighted by likelihoods. Intuitively, this method estimates the target location in the current frame by finding pixels likely belonging to the target region from the surrounding patch of the target location in the previous frame. Note that the likelihood of each particle can be an arbitrary function. Because of this flexibility, the particle filter-based tracking method can be adjusted to be suitable for a wide variety of tracking problems.

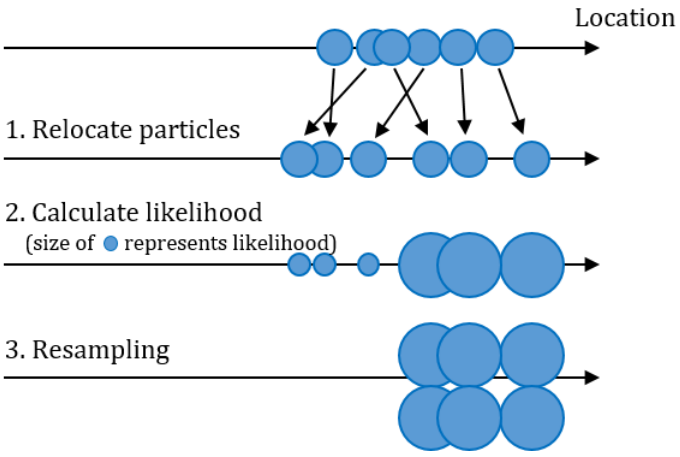

Fig. 2. Fundamental procedures in particle filter-based tracking method.

3. Tracking and Analysis of FUCCI Cells

We propose a method to track FUCCI cells and estimate the cell cycle phase based on particle filters. Additionally, we apply multistate time-to-event analysis to the results of our tracking and estimation method.

3.1. Tracking and State Estimation of FUCCI Cells Using a Particle Filter

3.1.1. Problem settings

In this study, each video to track is composed of the red fluorescence channel, the green fluorescence channel, and DIC image channel. An example of the data is shown in Fig. 1 (a). The goal is to predict the locations and "states" of each cell for each frame in a given video. As shown in Fig. 1 (b), FUCCI cells in the S phase and G2 phase have a similar green color and are difficult to distinguish. In addition, because the purpose of FUCCI cell tracking in this study is to analyze the relationship between time and the cell cycle progression, we do not have to distinguish the mitosis phase and cell death, which are both the ends of the cell cycle. Moreover, to avoid keeping tracking in the background region, our method should detect such tracking failure as a situation different from the regular tracking. Therefore, we do not estimate the phase itself and alternatively estimate the "state" determined by the color. Here, we define the state set as "G1" (red, same as G1), "eS" (yellow, early S), "S-G2" (green, S to G2), "M/D" (no fluorescence, M or cell death), and "TF" which stands for tracking failure.

3.1.2. Overview of our method

Our method tracks FUCCI cells based on particle filters. Because the color of FUCCI cells greatly changes according to the state, the state should be utilized for the definition of likelihood. This means that when calculating the likelihood of each particle, the state of the target cell in the previous frame is required. Therefore, our method iterates state estimation and location estimation using a particle filter (tracking) alternately. Section 3.1.4 describes our state estimation method, and Section 3.1.5 describes our tracking using the estimated state. The entire procedure of our method is as follows.

1) Preprocess the DIC channel image to separate the foreground (cell regions) and background (Section 3.1.3).
2) Detect the cells in the first frame and initialize trackers for each cell (Section 3.1.4).
3) Track each cell based on a particle filter. Iterate the following steps for each tracker in each frame.

a) Estimate the target cell's state (Section 3.1.5).
b) If the target cell's state remains "M/D" for a certain number of frames $m_{\text{"M/D"}}$, try to start tracking

daughter cells (Section 3.1.8).

c) Relocate the particles as described in Section 2.

d) Calculate the likelihood for each particle (Section 3.1.6).

e) Exclude particles violating the mutual exclusion constraint to deal with densely located cells (Section 3.1.7).

f) Resample the particles as described in Section 2.

3.1.3. Preprocessing of the DIC images

As discussed in Section 2, "M/D" cells do not emit both green and red fluorescence. In that state, the cell regions (foreground) and other regions (background) are difficult to distinguish in fluorescence images, and cell tracking is quite difficult. On the other hand, the appearance (texture) of cells in the DIC image does not change greatly, and thus, the DIC channel can be used to distinguish between the foreground and the background. However, the foreground and the background are difficult to distinguish in raw DIC images because of the low contrast. Therefore, our method preprocesses the DIC channel of the input video before tracking the cells. Fig. 3 shows the preprocessing procedure. In the cell regions of DIC images (Fig. 3 (a)), the spatial intensity change is much larger than that in other regions. Therefore, our method applies a differential filter to DIC images to emphasize the cell regions (Fig. 3 (b)). Then, our method binarizes the differential image (Fig. 3 (c)) and applies morphological operations and contour filling to outline the cell regions with contours (Fig. 3 (d)).

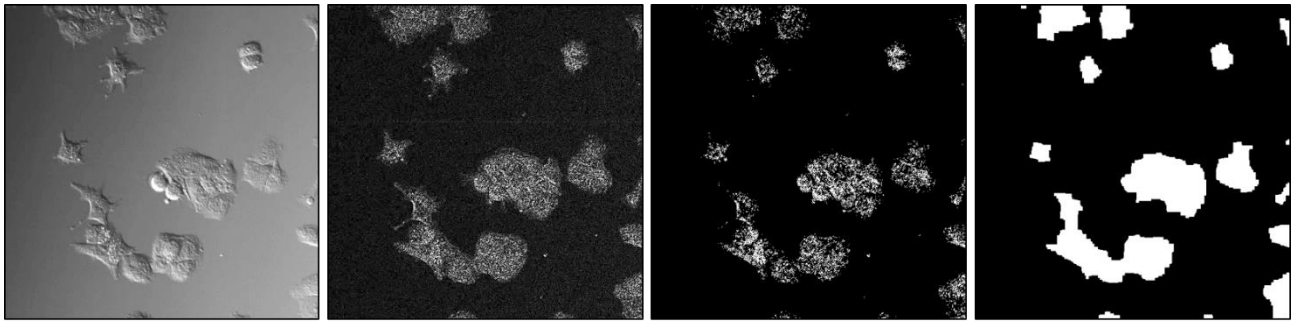

(a) Raw DIC image (b) Applying a differential filter (c) Binarization (d) Morphologial operations and contour filling

Fig. 3. Preprocessing of a DIC image (contrast enhanced).

3.1.4. Initialization of trackers

To initialize trackers, our method detects cells in the first frame using an arbitrary segmentation method. Then, our method locates trackers at the centers of segmented regions. A tracker is composed of a certain number of particles. Each particle has the following information.

1) $p_t^{(p)} = \left(x_t^{(p)}, y_t^{(p)}\right)$: The location of the particle in frame t.

2) $c_t^{(p)}$: The color at the particle's location $p_t^{(p)}$ in frame t.

3) $s_t^{(p)}$: The estimated state of the particle in frame t.

The estimation of $s_t^{(p)}$ is described in the next section. Each tracker (not each particle) also has information about the target cell as follows.

1) $p_t^{(c)} = \left(x_t^{(c)}, y_t^{(c)}\right)$: The estimated center location of the target cell in frame t.

2) $c_t^{(c)}$: The color at the target location $p_t^{(c)}$ in frame t.

3) $s_t^{(c)}$: The estimated state of the target cell in frame t.

Here, $p_t^{(c)}$ is calculated as the average of each particle's location $p_t^{(p)}$ weighted by the likelihood. $s_t^{(c)}$ is calculated as the majority of each particle's state $s_t^{(p)}$ weighted by the likelihood.

3.1.5. Estimation of cell states

The state $s_t^{(c)}$ of each cell is estimated as the weighted majority of each particle's state $s_t^{(p)}$, as mentioned in the previous section. To estimate each particle's state, our method utilizes the current color $c_t^{(p)}$ at the particle's location $p_t^{(p)}$. First, if the particle is located out of the cell region (i.e., located in the background), the particle is likely to have failed to capture the cell location. Therefore, if the intensity of the preprocessed DIC channel at the particle location is 0, the state of the particle is estimated as "TF". Second, if the particle location is inside the foreground but not enough fluorescence is observed there, the state of the particle is estimated as "M/D". That is, if the sum of the intensity of green channel and red channel is below the threshold τ, the state is estimated as "M/D". Then, to determine if the state is "G1" (red), "eS" (yellow), or "S-G2" (green), we use the hue in the HSV color space at the particle location. If the hue is sufficiently small (i.e., smaller than the threshold $\tau_{\text{"G1"}}$), the state is estimated as "G1". If the hue is sufficiently large (i.e., larger than the threshold $\tau_{\text{"S-G2"}}$), the state is estimated as "S-G2". If the hue does not satisfy either conditions above, the state is estimated as "eS".

3.1.6. Likelihood function

Our method calculates the likelihood of each particle using the information about the particle in the current frame t, i.e., $p_t^{(p)}$, $c_t^{(p)}$, and $s_t^{(p)}$, and the information about the target in the previous frame $t-1$, i.e., $p_{t-1}^{(c)}$, $c_{t-1}^{(c)}$, and $s_{t-1}^{(c)}$. The likelihood function is the product of three factors referred to as the state transition factor $l_S\left(s_{t-1}^{(c)}, s_t^{(p)}\right)$, the color factor $l_C\left(s_{t-1}^{(c)}, c_{t-1}^{(c)}, c_t^{(p)}\right)$, and the distance factor $l_D\left(p_{t-1}^{(c)}, p_t^{(p)}\right)$.

3.1.6.1. State transition factor

The state transition factor represents the naturalness of the state transition between the previous and current frames. In particular, the state transition factor is as follows. If $s_t^{(p)} = \text{"TF"}$ (tracking failure), the particle location is unlikely to belong to the target region. Thus, we define $l_S\left(s_{t-1}^{(c)}, \text{"TF"}\right) = \delta$, where δ is a small constant to avoid division by zero. In other cases, if the particle location belongs to the target region, the current state $s_t^{(p)}$ of the particle is likely to be the same as the previous state $s_{t-1}^{(c)}$ or the next state of $s_{t-1}^{(c)}$. Thus, in the case of $s_{t-1}^{(c)} \in \{\text{"G1"}, \text{"eS"}, \text{"S-G2"}\}$, we define the state transition factor as follows.

$$l_S\left(s_{t-1}^{(c)}, s_t^{(p)}\right) = \begin{cases} \alpha & \left(s_t^{(p)} = s_{t-1}^{(c)}\right) \\ 1-\alpha & \left(s_t^{(p)} = n\left(s_{t-1}^{(c)}\right)\right) \\ \delta & (\text{otherwise}) \end{cases} \quad (1)$$

where $0 < \alpha < 1$ is a constant and function n returns the next state of the given state, i.e., $n(\text{"G1"}) = \text{"eS"}$, $n(\text{"eS"}) = \text{"S-G2"}$, and $n(\text{"S-G2"}) = \text{"M/D"}$. If $s_{t-1}^{(c)} = \text{"M/D"}$, we define the state transition factor as α when $s_t^{(p)} = s_{t-1}^{(c)} = \text{"M/D"}$; otherwise $1-\alpha$. That is, cells in the "M/D" state are likely to stay in that state or to change into other states. Because particles are likely to get into the "M/D" state by mistake due to the temporally lower fluorescence intensity, our method allows such particles to return to the correct state.

3.1.6.2. Color factor

The color factor represents the naturalness of color change between the previous and current frames. First, if the particle is located in the background, $l_C\left(s_{t-1}^{(c)}, c_{t-1}^{(c)}, c_t^{(p)}\right) = \delta$. If the previous state $s_{t-1}^{(c)}$ of the

target cell is "G1" or "eS", we define the likelihood as $l_C\left(s_{t-1}^{(c)}, c_{t-1}^{(c)}, c_t^{(p)}\right) \approx 1$ when the color change between frames (i.e., difference between $c_{t-1}^{(c)}$ and $c_t^{(p)}$) is in the likely range; otherwise, the likelihood is smaller. To represent this behavior as the likelihood, we use the following functions.

$$f_1(x|v) = \frac{1}{1+\exp(x-v)} \tag{2}$$

$$f_2(x|v_l, v_r) = \min\left(f_1(-x|-v_l), f_1(x|v_r)\right) \# \tag{3}$$

Fig. 4 visualizes these functions. As shown in the figure, v in function f_1 denotes the inflection point satisfying $f_1(v \mid v) = 0.5$. Similarly, v_l and v_r in the function f_2 are inflection points satisfying $f_2(v_l \mid v_l, v_r) = f_2(v_r \mid v_l, v_r) = 0.5$.

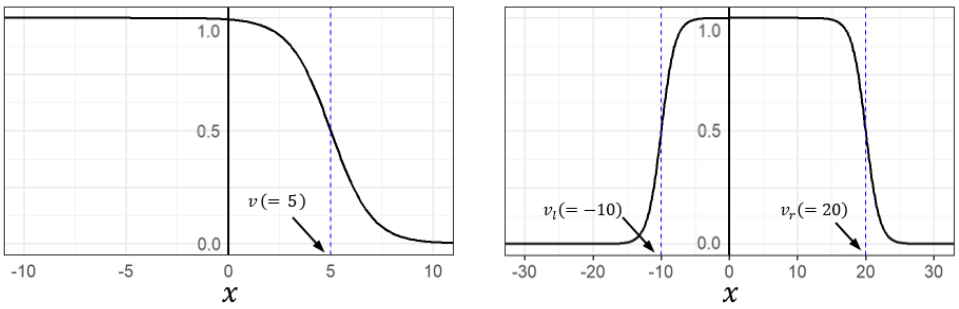

(a) $f_1(x \mid v)$, where $v = 5$ (b) $f_2(x \mid v_l, v_r)$, where $v_l = -10, v_r = 20$

Fig. 4. Function f_1 and function f_2.

In this study, we use the difference in the hue of the HSV color space to represent the color change between frames. The color change from the "G1" state (red) to the "S-G2" state (green) via the "eS" state (yellow) is described as the increase in the hue as shown in Fig. 5.

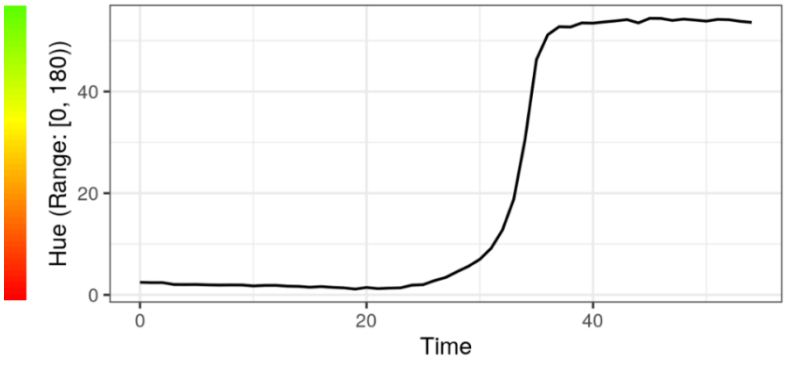

Fig. 5. A typical transition of the hue from the "G1" state to the "S-G2" state.

Compared to using the red and green channels, using the hue to represent color changes is relatively simpler. In addition, we consider that the hue is robust to variations in fluorescence intensity among target cells. That is, while the variations in fluorescence intensity directly affect the red and green channels, in the HSV color space, such variations mainly affect the brightness or value (V of HSV). Here, we define h as a function to convert a color in our method's color space (red, green, and preprocessed DIC) to the hue while

regarding the third channel as 0. Using this function, we define the color factor where $s_{t-1}^{(c)} \in$ {"G1", "eS"} as follows.

$$l_C\left(s_{t-1}^{(c)}, c_{t-1}^{(c)}, c_t^{(p)}\right) = f_2\left(h\left(c_t^{(p)}\right) - h\left(c_{t-1}^{(c)}\right) \middle| \beta_{s_{t-1}^{(c)}}^{(l)}\left(c_{t-1}^{(c)}\right) - \gamma,\ \beta_{s_{t-1}^{(c)}}^{(r)}\left(c_{t-1}^{(c)}\right) + \gamma\right) \tag{4}$$

where $\beta_s^{(l)}$ and $\beta_s^{(r)}$ are functions representing the likely upper and lower bounds of the hue change between current and previous frames, for the previous state s and the given previous hue. γ is a constant representing the distance between the lower or upper bound and the nearest infection points.

For the case of $s_{t-1}^{(c)} =$ "S-G2", the current state of the target cell is likely to be "S-G2" or "M/D". Therefore, the current color at the target location is likely to be the same as the target's previous color (green) or black (which means fluorescence disappearance). In such cases, the color factor of the likelihood should be calculated using not only the difference in the hue. Here, we use the sum of the red and green channels as in our state estimation (Section 3.1.5). We denote r and g as the functions to extract the red channel and the green channel, respectively, from the given color. Using these functions, we define the color factor in the case of $s_{t-1}^{(c)} =$ "S-G2" as follows.

$$l_C\left("\text{S-G2}", c_{t-1}^{(c)}, c_t^{(p)}\right)$$
$$= \frac{f_2\left(h\left(c_t^{(p)}\right) - h\left(c_{t-1}^{(c)}\right) \middle| \beta_{"\text{S-G2}"}^{(l)}\left(c_{t-1}^{(c)}\right) - \gamma, \beta_{"\text{S-G2}"}^{(r)}\left(c_{t-1}^{(c)}\right) + \gamma\right) + f_1\left(r\left(c_t^{(p)}\right) + g\left(c_t^{(p)}\right) \middle| \tau_{"\text{M/D}"} + \gamma\right)}{2} \tag{5}$$

In this study, the function $\beta_s^{(l)}$ is defined as 0 for any $s \in$ {"G1", "eS", "S-G2"} and given previous hue. This is because the hue is not likely to decrease greatly when the previous state s is "G1", "eS", or "S-G2", as shown in Fig. 5. The function $\beta_s^{(r)}$ is defined as the difference between the likely upper bound of the current hue and the given previous hue. Therefore, we define $\beta_s^{(r)}$ as follows.

$$\beta_s^{(r)}(c) = \xi_s - h(c) \tag{6}$$

where ξ_s is the likely upper bound of the current hue for the previous state s.

For the remaining case of $s_{t-1}{}^{(c)}$ is "M/D", we define the color factor as

$$l_C\left("\text{M/D}",\ c_{t-1}^{(c)},\ c_t^{(p)}\right) = \begin{cases} \varepsilon & \left(d\left(c_t^{(p)}\right) = 1\right) \\ \delta & (\text{otherwise}) \end{cases} \tag{7}$$

where $0 < \varepsilon < 1$ is a constant and d is a function to extract the preprocessed DIC channel from the given color and normalize the value in [0, 1].

3.1.6.3. Distance factor

The distance factor represents the closeness between the current particle location $p_{t-1}^{(c)}$ and the previous cell location $p_t^{(p)}$. We define this factor so that the value is higher if the distance between $p_{t-1}^{(c)}$ and $p_t^{(p)}$ is smaller than half of the approximate cell width and decreases as the distance increases, as follows.

$$l_D\left(p_{t-1}^{(c)}, p_t^{(p)}\right) = f_1\left(e\left(p_{t-1}^{(c)}, p_t^{(p)}\right) \middle| \lambda + \gamma\right) \tag{8}$$

where e is a function to calculate the Euclidean distance between two given locations and λ is half of the approximate cell width.

3.1.7. Mutual Exclusion Constraint

In particle filter-based tracking, the target location is estimated by sampling around the previous target location and weighting samples according to their likelihood. This policy can lead to failure when cells are densely located. If two cells A and B, with similar appearances (e.g., colors in the case of FUCCI cells), are close to each other, the particle locations of the trackers for each cell can overlap. Because cells A and B are similar in appearance, the likelihood of particles is high even if the particle is inside another cell. In this situation, tracking of both cells is prone to failure. Therefore, we apply the mutual exclusion constraint [12] for all trackers. In the mutual exclusion constraint, a particle is excluded from the tracker if the particle's likelihood increases when it is calculated supposing that the particle belongs to another tracker. By applying this constraint, particles likely in other target regions are excluded and not utilized for the location estimation.

3.1.8. Detection of Cell Division and Death

When the state of the target cell of some tracker continues being "M/D" for a certain number $m_{\text{"M/D"}}$ of time steps, our method stops the tracker from relocating and resampling the particles and starts to detect daughter cells in the "G1" state around the tracker's current location $p^{(c)}$. Waiting for $m_{\text{"M/D"}}$ steps is necessary because cells can be determined as in the "M/D" state due to the temporally lower fluorescence intensity. Detection is conducted in the patch around $p^{(c)}$ using the following algorithm.

1) Binarize the red channel image after smoothing with an averaging filter.
2) Extract cell regions in the red channel image, which are also in the foreground region of the preprocessed DIC channel image.
3) Apply the watershed algorithm to separate connected foregrounds.

If two or more cells are detected, then our method excludes cells already tracked by other trackers from the detected set. Specifically, if a detected cell's location is closer to the center of some "G1" cell tracked by another tracker than $p^{(c)}$, the detected cell is excluded. If two or more cells remain, two cells closest to $p^{(c)}$ are determined as the daughter cells. Once the daughter cells are detected, our method stops tracking the parent cell and starts tracking the daughter cells using new trackers; otherwise, our method iterates the above procedure in the next frame. If daughter cells are not detected in m_{D} time steps, our method determines that cell death occurred and stops tracking the cell.

3.2. Time-to-Event Analysis

The results of tracking and estimating states of FUCCI cells include sequences of states and occupation time for each phase. However, some of the results also include the uncertainty of state transition after the final frame or the tracking failure. For such complicated data, visualizing the sequences of states over time does not help derive a reliable conclusion. Therefore, we propose to apply multistate time-to-event (TTE) analysis [13] on such sequences. TTE analysis, also referred to as event-history analysis and survival analysis, estimates the probability of occurrence of "events," which are experiences of interest such as death of patients and failure of machines.

An important feature of TTE analysis is the concept of censoring. If some individual observations cannot provide information about the occurrence time of the event, the observation is censored. If we observe patient deaths as events, the following data are all censored: data about a patient who does not die before the end of observation, data about a patient who dies because of unexpected causes, and data about a patient whose observation is canceled due to transfer. In TTE analysis, censored data are not ignored but

handled differently.

TTE analysis utilized in this paper is an extended version of TTE analysis called multistate TTE analysis. In multistate TTE analysis, surviving targets progress toward the event via multiple different states using a multistate model with inter-state transition. Functions estimated in multistate TTE analysis include state occupation probabilities for each state over time and inter-state transition probabilities. In this paper, we apply multistate TTE analysis on the tracking results of FUCCI cells to analyze the difference in the cell cycle progression between samples with medicine administration and those without. In our analysis, the sequence that includes the end of observation or tracking failure is censored.

4. Experimental Results

4.1. Data

We applied our method to time-lapse videos of FUCCI-labeled HuH7 cells (human hepatocellular carcinoma cell line). These videos were taken at 30 min intervals over approximately 3 days (total of 150 frames). The red and green fluorescence images were obtained at $1{,}024 \times 1{,}024$ pixel resolution and 12-bit (4,096 gradations) dynamic range. We used two datasets. The first one is composed of 10 visual fields of control (without medicine administration). The second one is composed of 10 visual fields with interferon-α administration. Interferon-α is a medicine used to treat liver cancers clinically.

4.2. Implementation

We implemented our tracking method using the Python language with the OpenCV library. We determined the parameters in our method heuristically. Specifically, parameters τ_s for $s \in$ {"G1", "S-G2", "M/D"} (thresholds for estimating the cell state from the hue) were determined using the averaged sequence of color transition in an annotated visual field. Parameters ξ_s for $s \in$ {"G1", "eS", "S-G2"} (the upper bound of the likely current hue for the previous state s) were defined as follows. $\xi_{\text{"G1"}}$ and $\xi_{\text{"eS"}}$ are the averaged hue in the state "eS" and "S-G2", respectively. $\xi_{\text{"S-G2"}}$ is the maximum hue in the state "S-G2". Each specific value was derived from an annotated visual field. In addition, we used the seeded-growth algorithm for segmentation of the first frame. This algorithm is also used in the LineageTracker plugin [5] of ImageJ [14], and we obtained the segmentation results through that plugin.

In the experiment to compare the tracking performance (Section 4.3), we used LineageTracker and LAP tracker as well as our method. We used the LineageTracker plugin of ImageJ and the TrackMate [15] plugin of Fiji [16], a distribution of ImageJ, which provides LAP tracker as an option.

We performed our multistate TTE analysis using the R language and the msSurv package [13].

4.3. Evaluation of Tracking

To evaluate the performance of our method, we utilized 2 annotated visual fields. Visual field #1 was also used for parameter setting. We applied our method, LineageTracker, and LAP tracker to these videos and compared the results. We tuned the parameter settings in LineageTracker and LAP tracker manually for the fair comparison.

4.3.1. Evaluation criteria

A simple criterion to evaluate the performance of tracking is the accuracy. This criterion evaluates how many objects are detected in each frame on average as a comparison with the ground-truth. The accuracy of tracking a for a tracking result (i.e., a set of obtained trajectories) is calculated as follows.

$$a = \frac{1}{f}\sum_t \frac{d_t}{n_t} \tag{9}$$

where f is the number of frames, n_t is the number of cells in the frame t of the ground-truth, and d_t is the number of successfully detected cells in the frame t. Here, we say a cell is successfully detected in the frame t if the distance between the cell and one of the obtained trajectories in the frame t is below the threshold. In this experiment, we defined this threshold as half of the approximate cell width, specifically 20 pixels. Obviously, accuracy is higher for better performance.

The accuracy can be used to evaluate how many cells are detected in each frame from its definition above. However, in FUCCI cell tracking, tracking each cell for consequent frames is more important than tracking many cells. Therefore, we used other criteria to evaluate how many frames the tracking method can track the same target. One criterion is MT (Mostly Tracked) [17], which means the rate of mostly tracked trajectories, i.e., ground-truth trajectories that are tracked as the same target at least 80% frames of their life span. Here, "tracked" means that the location error is 20 pixels or less, similar to the calculation of accuracy. Another criterion is ML (Mostly Lost) [17], which means the rate of mostly lost trajectories, i.e., ground-truth trajectories that are tracked at most 20% frames of their life span. MT is higher and ML is lower for better performance.

4.3.2. Results

Table 1 shows the tracking results of both our method and LineageTracker evaluated in terms of accuracy, MT and ML. Higher values denote better performance in criteria with (↑), and lower values denote better performance in criteria with (↓). For LineageTracker and LAP tracker, both the best results obtained through parameter tuning and the results with default settings (in parentheses) are shown. The best result for each criterion is written in bold font.

Table 1. Tracking Results for Each Visual Field

	Visual field #1			Visual field #2		
	Accuracy (↑)	MT (↑)	ML (↓)	Accuracy (↑)	MT (↑)	ML (↓)
Our method	0.611	**0.302**	**0.238**	0.638	**0.400**	**0.200**
LineageTracker	0.821 (0.821)	0.081 (0.024)	0.551 (0.700)	0.938 (0.938)	0.109 (0.042)	0.611 (0.733)
LAP tracker	**0.891** (0.841)	0.092 (0.008)	0.637 (0.714)	**0.946** (0.884)	0.093 (0.055)	0.629 (0.664)

As a result, our method achieved better performance in terms of the MT and ML criteria for both data. Thus, we confirmed that our method is more capable of continuously tracking FUCCI cells for longer time steps than existing methods. In terms of the accuracy, LineageTracker and LAP tracker achieved better performance for both visual fields. This result is reasonable. While LineageTracker and LAP tracker, which are detection-based tracking methods, conduct segmentation for all frames first, our method tracks only the cells detected in the first frame and the daughter cells detected in the later frames. Therefore, LineageTracker and LAP tracker are capable of detect more cells, compared to our method. However, in FUCCI cell tracking, continuously tracking the same target is more important than tracking many targets. Therefore, this result shows the effectiveness of our method for FUCCI cell tracking.

Fig. 6 shows the example results of our tracking method. In each example, small circles in the images represent the locations of particles, and large circles in each image represent the locations of target cells. The images on the right in each example are DIC images superimposed with particle and cell locations. Here, the color of each circle represents the state of the particle or cell as follows; the red color corresponds to "G1", the yellow color corresponds to "eS", the green color corresponds to "S-G2", the blue color corresponds to "M/D", and the black color corresponds to "TF". The images on the right in each example depict red and green fluorescence with cell locations in white color. In Fig. 6 (a), although there are some areas where

multiple cells are densely located, each cell with red and green fluorescence is tracked correctly. In Fig. 6 (b), the tracker tracks the target cell 34 in frame 60 (top); however, it tracks a different cell in frame 68 (bottom). The reason for this mistracking is that the cell tracked in frame 68 is not originally tracked by other trackers. In such cases, even though our method utilizes the mutual exclusion constraint, the tracker has the possibility to erroneously track the untargeted cell whose likelihood is sufficiently high because it has a similar appearance.

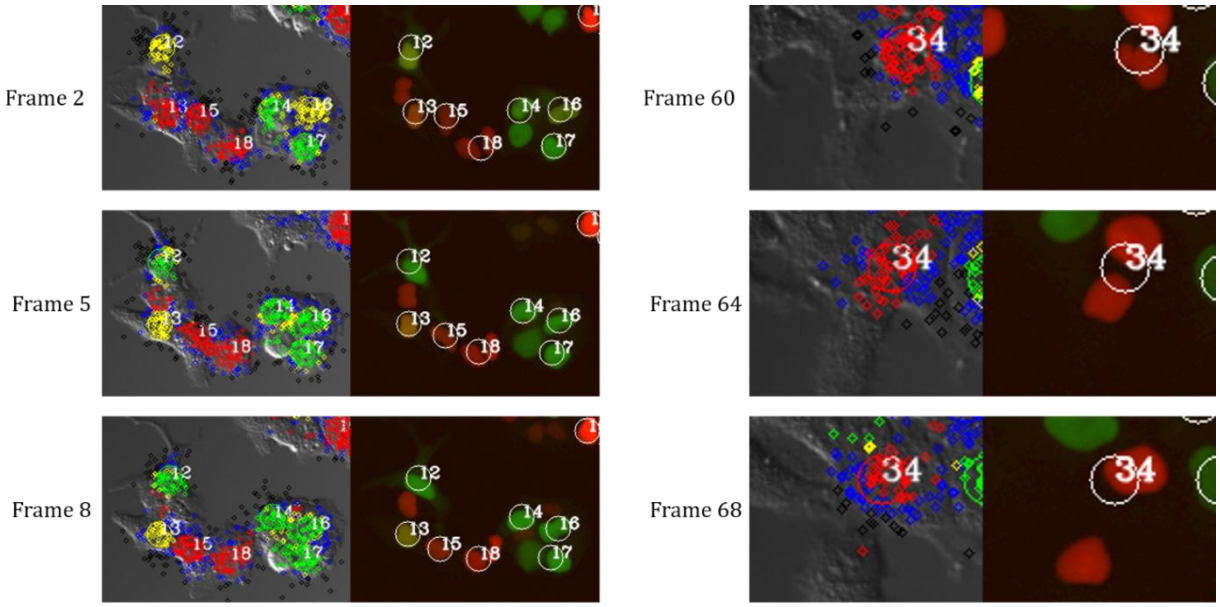

Fig. 6. Example results of our tracking method (contrast enhanced).

4.4. Multistate Time-to-Event Analysis

We applied multistate TTE analysis to the results of our method using whole 20 visual fields, including non-annotated visual fields. Fig. 7 shows the state occupancy probabilities for both groups of cells under control and interferon-administered conditions. In Fig. 7, the blue and red bands surrounding the plotted line represent the 95% confidence intervals. As shown on the left in Fig. 7, the state occupation probabilities of the G1 phase under the interferon-administered condition are higher than the probabilities under the control condition. This result suggests that a relatively larger number of cells tend to keep staying in the G1 phase (i.e., unable to progress to the S phase) compared to the cells in the control condition. This phenomenon is known as G0/G1 arrest [18].

5. Discussion and Future Work

5.1. Improving the Tracking Method for FUCCI cells

In the experimental results shown in Fig. 6 (b), our tracker loses the target even though the cells are not densely located. This is because the likelihood of particles in the neighbor untargeted cell region is sufficiently high, as the target and neighbor cells are quite similar. Although our method employs the mutual exclusion constraint to exclude such particles, it is not valid if the neighbor cell is not tracked by any trackers. One of the straightforward ways to solve this problem is to track all cells in the visual field. However, tracking all cells requires segmentation for every frame. While image segmentation is a well-studied problem, accurate segmentation of bioimages with low S/N ratios, low contrast, densely

located targets and a large number of highly similar targets is still challenging. Therefore, a more accurate tracking method that does not depend on the segmentation performance is required. One of our ideas is to utilize the history of each target's motion as auxiliary information. Specifically, we are considering adaptively adjusting the particle filter settings, such as the number of particles, the distribution of displacements to add to the particle locations for relocation, and the design of the likelihood function. Using the history of the target's motion, our method can estimate the location of the target with features unique to the target itself and has possibilities to achieve more accurate tracking.

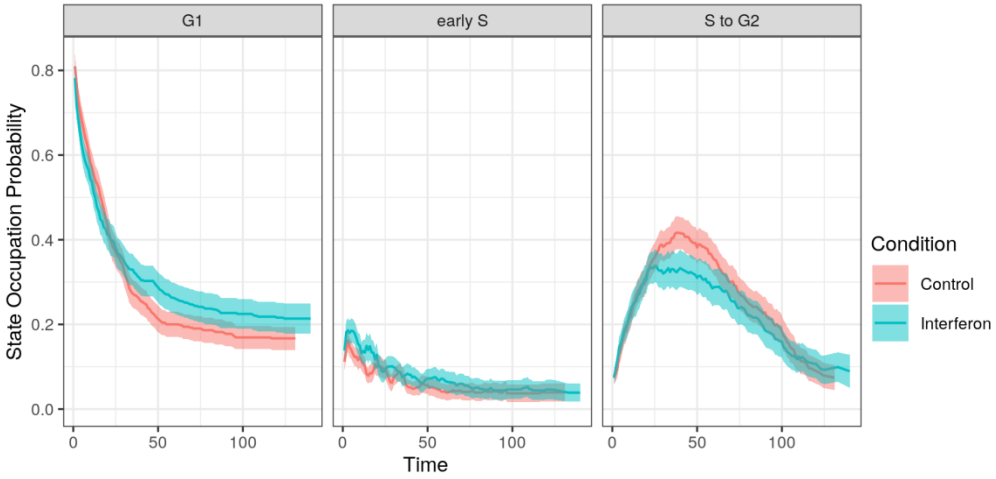

Fig. 7. State occupation probabilities obtained through multistate TTE analysis.

In this paper, our method does not distinguish between the mitosis phase and cell death. However, for some kind of analysis, these two events should be separately handled. For example, a kind of anti-cancer agent induces apoptosis in cancer cells, while another agent inhibits metastasis and proliferation of cancer cells. Discrimination between the mitosis and cell death is important for evaluating the effects of combination chemotherapy when both kinds of agents are used.

5.2. Analysis of the Cell Cycle via Cell Tracking and TTE Analysis

In our TTE analysis, we confirmed that our method for tracking and estimating cell state produces useful data for the analysis of the cell cycle. Our results of TTE analysis in Fig. 7 do not show a great difference between the two conditions. Such a small but significant difference is difficult to reveal without TTE analysis. Quantification via visual inspection is unrealistic in situations with a large number of cells, frames, visual fields, and/or conditions. Therefore, our method can be an effective way to extract useful information about the transitions of cell states from time-lapse videos.

6. Conclusion

In this paper, we proposed a method to track and estimate the states of FUCCI cells for analysis of the cell cycle. Our method tracks the target cells based on particle filters and simultaneously estimates their states. We showed that our method achieves much better performance in terms of continuous tracking of the target cell, which is important for the analysis of the cell cycle, compared to existing detection-based tracking methods. Additionally, we confirmed the usefulness of TTE analysis of the tracking results. Our method effectively handles enormous amount of time-lapse videos obtained through temporal observation on fluorescently labeled cells.

Conflict of Interest

The authors declare no conflict of interest.

Author Contributions

KF and SS designed the study, implemented the algorithm and performed the analyses; MI provided the data and discussed the results; HS, TM, and HM contributed to improving the algorithm; KF and SS wrote the manuscript draft; HM supervised the study; all authors had approved the final version.

Acknowledgment

The authors would like to thank Dr. Junichi Kikuta, Dr. Yoshinori Kagawa, and Dr. Sakae Maeda for the insightful suggestions. This work was supported in part by JST CREST Grant Number JPMJCR15G1; JSPS KAKENHI Grant Number JP18H05035, JP18K19842, and JP19H04207, Japan.

References

[1] Usaj, M. M., Styles, E. B., Verster, A. J., Friesen, H., Boone, C., & Andrews, B. J. (2016). High-content screening for quantitative cell biology. *Trends in cell biology, 26(8)*, 598-611.

[2] Zielke, N., & Edgar, B. A. (2015). FUCCI sensors: powerful new tools for analysis of cell proliferation. *Wiley Interdisciplinary Reviews: Developmental Biology, 4(5)*, 469-487.

[3] He, T., Mao, H., Guo, J., & Yi, Z. (2017). Cell tracking using deep neural networks with multi-task learning. *Image and Vision Computing, 60*, 142-153.

[4] Hayashida, J., & Bise, R. (2019). Cell tracking with deep learning for cell detection and motion estimation in low-frame-rate. *Proceedings of International Conference on Medical Image Computing and Computer-Assisted Intervention* (pp. 397-405). Shenzhen: the MICCAI Society.

[5] Downey, M. J., Jeziorska, D. M., Ott, S., Tamai, T. K., Koentges, G., Vance, K. W., & Bretschneider, T. (2011). Extracting fluorescent reporter time courses of cell lineages from high-throughput microscopy at low temporal resolution. *PloS one, 6(12)*, e27886.

[6] Jaqaman, K., Loerke, D., Mettlen, M., Kuwata, H., Grinstein, S., Schmid, S. L., & Danuser, G. (2008). Robust single-particle tracking in live-cell time-lapse sequences. *Nature methods, 5(8)*, 695.

[7] Yuan, L., Zheng, Y. F., Zhu, J., Wang, L., & Brown, A. (2011). Object tracking with particle filtering in fluorescence microscopy images: Application to the motion of neurofilaments in axons. *IEEE Transactions on Medical Imaging, 31(1)*, 117-130.

[8] Tokunaga, T., Hirose, O., Kawaguchi, S., Toyoshima, Y., Teramoto, T., Ikebata, H., *et al*. (2014). Automated detection and tracking of many cells by using 4D live-cell imaging data. *Bioinformatics, 30(12)*, i43-i51.

[9] Shigeta, H., Seno, S., Nishizawa, S., Uchida, Y., Kikuta, J., Ishii, M., & Matsuda, H. (2019). Analyzing leukocyte migration trajectories by deformable image matching. *Proceedings of 2019 IEEE International Conference on Bioinformatics and BioEngineering* (pp. 94-98). Athens: IEEE.

[10] Padfield, D., Rittscher, J., & Roysam, B. (2011). Coupled minimum-cost flow cell tracking for high-throughput quantitative analysis. *Medical image analysis, 15(4)*, 650-668.

[11] Arulampalam, M. S., Maskell, S., Gordon, N., & Clapp, T. (2002). A tutorial on particle filters for online nonlinear/non-Gaussian Bayesian tracking. *IEEE Transactions on Signal Processing, 50(2)*, 174-188.

[12] Chai, Y., Park, J., Yoon, K., & Kim, T. (2011). Multi target tracking using multiple independent particle filters for video surveillance. *Proceedings of 2011 IEEE International Conference on Consumer Electronics* (pp. 735-736). Berlin: IEEE.

[13] Ferguson, N., Datta, S., & Brock, G. (2012). msSurv, an R package for nonparametric estimation of multistate models. *Journal of Statistical Software, 50(14)*, 1-24.

[14] Schneider, C. A., Rasband, W. S., & Eliceiri, K. W. (2012). NIH image to ImageJ: 25 years of image analysis.

Nature Methods, 9(7), 671.

[15] Tinevez, J. Y., Perry, N., Schindelin, J., Hoopes, G. M., Reynolds, G. D., Laplantine, E., Bednarek, S. Y., Shorte, S. L., & Eliceiri, K. W. (2017). TrackMate: An open and extensible platform for single-particle tracking. *Methods, 115*, 80-90.

[16] Schindelin, J., Arganda-Carreras, I., Frise, E., Kaynig, V., Longair, M., Pietzsch, T., Preibisch, S., Rueden, C., Saalfeld, S., Schmid, B., Tinevez, J. Y., White, D. J., Hartenstein, V., Eliceiri, K., Tomancak, P., & Cardona, A. (2012). Fiji: An open-source platform for biological-image analysis. *Nature Methods, 9(7)*, 676-682.

[17] Yoon, J. H., Yang, M. H., Lim, J., & Yoon, K. J. (2015). Bayesian multi-object tracking using motion context from multiple objects. *Proceedings of 2015 IEEE Winter Conference on Applications of Computer Vision* (pp. 33-40). Waikoloa Beach, HI: IEEE.

[18] Maeda, S., Wada, H., Naito, Y., Nagano, H., Simmons, S., & Kagawa, Y., *et al*. (2014). Interferon-α acts on the S/G2/M phases to induce apoptosis in the G1 phase of an IFNAR2-expressing hepatocellular carcinoma cell line. *Journal of Biological Chemistry, 289(34)*, 23786-23795.

Kenji Fujimoto received his B.E. degree from Osaka University in 2019. He is currently a student in the master's course of the Department of Bioinformatic Engineering, Graduate School of Information Science and Technology, Osaka University. His research interests include bioimage informatics.

Shigeto Seno received his B.E., M.E., and Ph.D. (information science) degrees from Osaka University in 2001, 2003, and 2006, respectively. He has been an associate professor in the Department of Bioinformatic Engineering, Graduate School of Information Science and Technology, Osaka University, since 2017. His research interests include data mining, bioinformatics (gene expression analysis), and bioimage informatics. He is a member of IPSJ, JSBi, and MII.

Hironori Shigeta is an assistant professor of the Graduate School of Information Science and Technology, Osaka University. He was a specially appointed assistant professor (CREST, JST) at Osaka University from 2017 to 2019. He received his B.E., M.E., and Ph.D. degrees from Osaka University in 2008, 2010, and 2016, respectively. He is a member of IPSJ, VRSJ, and ACM.

Tomohiro Mashita graduated from Osaka University in 2001 and completed the M.S. and doctoral programs in 2003 and 2006, respectively. He was a postdoctoral fellow at Osaka University from 2006 to 2008. He was a senior research fellow at Graz University of Technology from 2012 to 2013. He is currently an associate professor at Cybermedia Center, Osaka University. His research interest includes computer vision, and pattern recognition. He is a member of the IEICE, IPSJ, VRSJ, and IEEE.

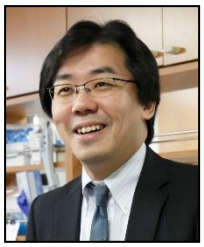

Masaru Ishii M.D., Ph.D. (professor of immunology and cell biology, Graduate School of Medicine and Frontier Biosciences, Osaka University) graduated from the Osaka University Medical School in 1998, and then worked as a physician specialized in rheumatology and internal medicine. He studied in the National Institutes of Health as a research fellow supported by the Human Frontier Science Program (2006–2008), as a Laboratory Chief in Osaka University Immunology Frontier Research Center (associate professor; 2008–2011, professor; 2011–2013), and then appointed as a professor and chairman of the Department of Immunology and Cell Biology, Graduate School of Medicine, Osaka University, since 2013. The bulk of his studies has so far elucidated the cellular dynamics in live bone tissues, with a special focus on bone-resorbing osteoclasts, by using intravital multiphoton-based bone imaging that he has originally developed. His study is not limited in the field of bone biology, but is currently covering diverse research topics where cells are dynamically moving, such as immune cell migration in inflammatory sites and cancer invasion/metastases.

Hideo Matsuda received his B.Sc. degree in physics from Kobe University, Japan, in 1982, and he received his M.E. and Ph.D. degrees in computer science from Kobe University, Japan, in 1984 and 1987, respectively. He has been a professor in the Department of Bioinformatic Engineering, Graduate School of Information Science and Technology, Osaka University, since 2002. His research interests include genomic data analysis, gene regulatory networks, and gene expression analysis. He is a member of JSBi, IPSJ, IEEE-CS, and ACM.